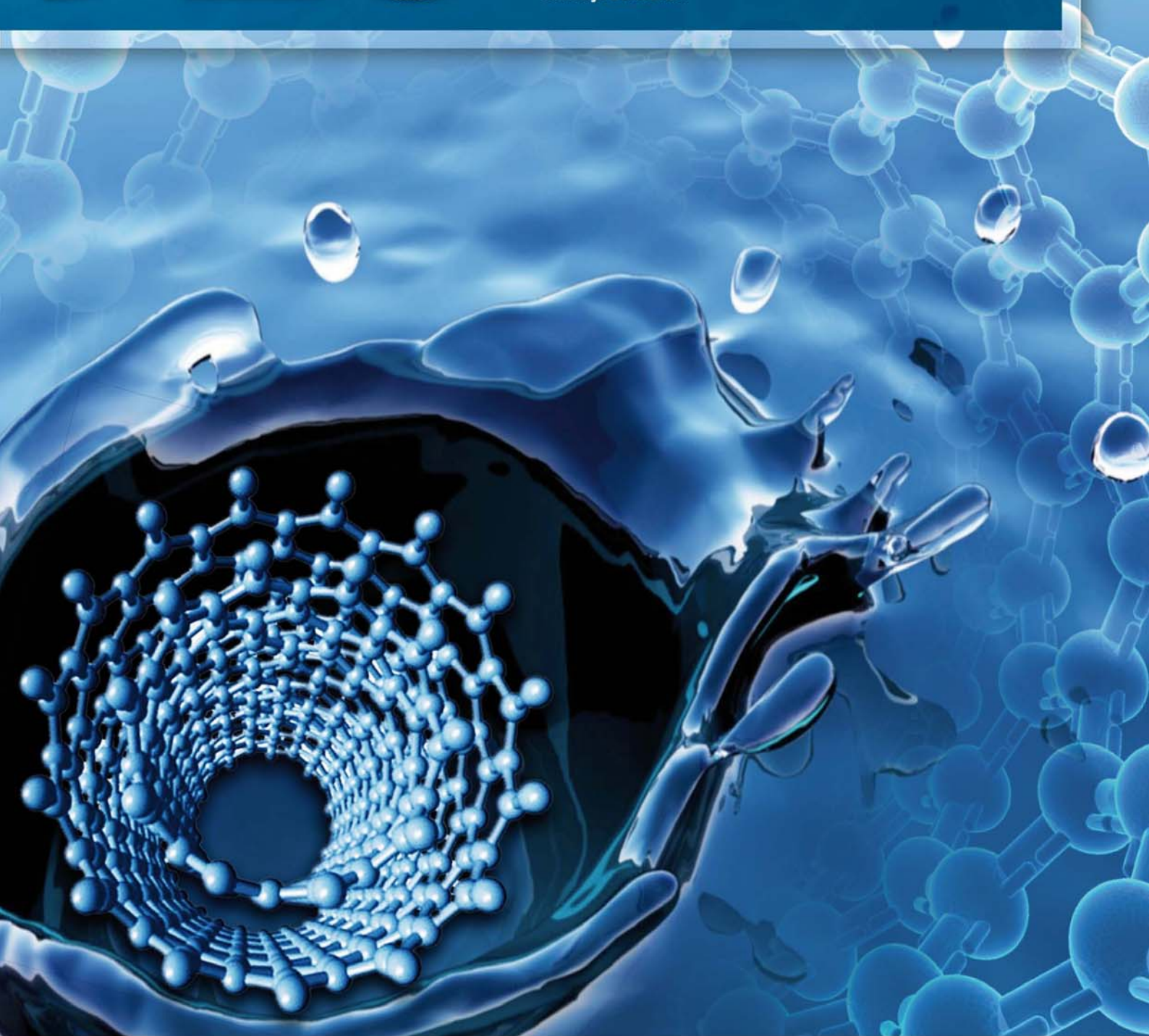


# JES

JOURNAL OF  
ENVIRONMENTAL  
SCIENCES

ISSN 1001-0742  
CN 11-2629/X

July 1, 2013 Volume 25 Number 7  
[www.jesc.ac.cn](http://www.jesc.ac.cn)



Sponsored by  
Research Center for Eco-Environmental Sciences  
Chinese Academy of Sciences

## CONTENTS

### Aquatic environment

- Application potential of carbon nanotubes in water treatment: A review  
Xitong Liu, Mengshu Wang, Shujuan Zhang, Bingcai Pan ..... 1263
- Characterization, treatment and releases of PBDEs and PAHs in a typical municipal sewage treatment plant situated beside an urban river, East China  
Xiaowei Wang, Beidou Xi, Shouliang Huo, Wenjun Sun, Hongwei Pan, Jingtian Zhang, Yuqing Ren, Hongliang Liu ..... 1281
- Factors influencing antibiotics adsorption onto engineered adsorbents  
Mingfang Xia, Aimin Li, Zhaolian Zhu, Qin Zhou, Weiben Yang ..... 1291
- Assessment of heavy metal enrichment and its human impact in lacustrine sediments from four lakes in the mid-low reaches of the Yangtze River, China  
Haijian Bing, Yanhong Wu, Enfeng Liu, Xiangdong Yang ..... 1300
- Biodegradation of 2-methylquinoline by *Enterobacter aerogenes* TJ-D isolated from activated sludge  
Lin Wang, Yongmei Li, Jingyuan Duan ..... 1310
- Inactivation, reactivation and regrowth of indigenous bacteria in reclaimed water after chlorine disinfection of a municipal wastewater treatment plant  
Dan Li, Siyu Zeng, April Z. Gu, Miao He, Hanchang Shi ..... 1319
- Photochemical degradation of nonylphenol in aqueous solution: The impact of pH and hydroxyl radical promoters  
Aleksandr Dulov, Niina Dulova, Marina Trapido ..... 1326
- A pilot-scale study of cryolite precipitation from high fluoride-containing wastewater in a reaction-separation integrated reactor  
Ke Jiang, Kanggen Zhou, Youcai Yang, Hu Du ..... 1331

### Atmospheric environment

- Effect of phosphogypsum and dicyandiamide as additives on NH<sub>3</sub>, N<sub>2</sub>O and CH<sub>4</sub> emissions during composting  
Yiming Luo, Guoxue Li, Wenhai Luo, Frank Schuchardt, Tao Jiang, Degang Xu ..... 1338
- Evaluation of heavy metal contamination hazards in nuisance dust particles, in Kurdistan Province, western Iran  
Reza Bashiri Khuzestani, Bubak Sourì ..... 1346

### Terrestrial environment

- Utilizing surfactants to control the sorption, desorption, and biodegradation of phenanthrene in soil-water system  
Haiwei Jin, Wenjun Zhou, Lizhong Zhu ..... 1355
- Detoxifying PCDD/Fs and heavy metals in fly ash from medical waste incinerators with a DC double arc plasma torch  
Xinchao Pan, Jianhua Yan, Zhengmiao Xie ..... 1362
- Role of sorbent surface functionalities and microporosity in 2,2',4,4'-tetrabromodiphenyl ether sorption onto biochars  
Jia Xin, Ruilong Liu, Hubo Fan, Meilan Wang, Miao Li, Xiang Liu ..... 1368

### Environmental biology

- Systematic analysis of microfauna indicator values for treatment performance in a full-scale municipal wastewater treatment plant  
Bo Hu, Rong Qi, Min Yang ..... 1379
- Function of *arsATorf7orf8* of *Bacillus* sp. CDB3 in arsenic resistance  
Wei Zheng, James Scifleet, Xuefei Yu, Tingbo Jiang, Ren Zhang ..... 1386
- Enrichment, isolation and identification of sulfur-oxidizing bacteria from sulfide removing bioreactor  
Jianfei Luo, Guoliang Tian, Weitie Lin ..... 1393

---

## Environmental health and toxicology

- In vitro* immunotoxicity of untreated and treated urban wastewaters using various treatment processes to rainbow trout leucocytes  
François Gagné, Marlène Fortier, Michel Fournier, Shirley-Anne Smyth ..... 1400
- Using lysosomal membrane stability of haemocytes in *Ruditapes philippinarum* as a biomarker of cellular stress  
to assess contamination by caffeine, ibuprofen, carbamazepine and novobiocin  
Gabriela V. Aguirre-Martínez, Sara Buratti, Elena Fabbri, Angel T. DelValls, M. Laura Martín-Díaz ..... 1408

## Environmental catalysis and materials

- Effect of transition metal doping under reducing calcination atmosphere on photocatalytic  
property of TiO<sub>2</sub> immobilized on SiO<sub>2</sub> beads  
Rumi Chand, Eiko Obuchi, Katsumi Katoh, Hom Nath Luitel, Katsuyuki Nakano ..... 1419
- A high activity of Ti/SnO<sub>2</sub>-Sb electrode in the electrochemical degradation of 2,4-dichlorophenol in aqueous solution  
Junfeng Niu, Dusmant Maharana, Jiale Xu, Zhen Chai, Yueping Bao ..... 1424
- Effects of rhamnolipid biosurfactant JBR425 and synthetic surfactant Surfynol465 on the  
peroxidase-catalyzed oxidation of 2-naphthol  
Ivanec-Goranina Rūta, Kulys Juozas ..... 1431

## The 8th International Conference on Sustainable Water Environment

- An novel identification method of the environmental risk sources for surface water pollution accidents in chemical industrial parks  
Jianfeng Peng, Yonghui Song, Peng Yuan, Shuhu Xiao, Lu Han ..... 1441
- Distribution and contamination status of chromium in surface sediments of northern Kaohsiung Harbor, Taiwan  
Cheng-Di Dong, Chiu-Wen Chen, Chih-Feng Chen ..... 1450
- Historical trends in the anthropogenic heavy metal levels in the tidal flat sediments of Lianyungang, China  
Rui Zhang, Fan Zhang, Yingjun Ding, Jinrong Gao, Jing Chen, Li Zhou ..... 1458
- Heterogeneous Fenton degradation of azo dyes catalyzed by modified polyacrylonitrile fiber Fe complexes:  
QSPR (quantitative structure property relationship) study  
Bing Li, Yongchun Dong, Zhizhong Ding ..... 1469
- Rehabilitation and improvement of Guilin urban water environment: Function-oriented management  
Yuansheng Pei, Hua Zuo, Zhaokun Luan, Sijia Gao ..... 1477
- Adsorption of Mn<sup>2+</sup> from aqueous solution using Fe and Mn oxide-coated sand  
Chi-Chuan Kan, Mannie C Aganon, Cybelle Morales Futalan, Maria Lourdes P Dalida ..... 1483
- Degradation kinetics and mechanism of trace nitrobenzene by granular activated carbon enhanced  
microwave/hydrogen peroxide system  
Dina Tan, Honghu Zeng, Jie Liu, Xiaozhang Yu, Yanpeng Liang, Lanjing Lu ..... 1492

Serial parameter: CN 11-2629/X\*1989\*m\*237\*en\*P\*28\*2013-7



## Heterogeneous Fenton degradation of azo dyes catalyzed by modified polyacrylonitrile fiber Fe complexes: QSPR (quantitative structure property relationship) study

Bing Li, Yongchun Dong\*, Zhizhong Ding

*Division of Textile Chemistry & Ecology, School of Textiles, Tianjin Polytechnic University, Tianjin 300387, China.  
E-mail: [bingli1010@sina.cn](mailto:bingli1010@sina.cn)*

### Abstract

The amidoximated polyacrylonitrile (PAN) fiber Fe complexes were prepared and used as the heterogeneous Fenton catalysts for the degradation of 28 anionic water soluble azo dyes in water under visible irradiation. The multiple linear regression (MLR) method was employed to develop the quantitative structure property relationship (QSPR) model equations for the decoloration and mineralization of azo dyes. Moreover, the predictive ability of the QSPR model equations was assessed using Leave-one-out (LOO) and cross-validation (CV) methods. Additionally, the effect of Fe content of catalyst and the sodium chloride in water on QSPR model equations were also investigated. The results indicated that the heterogeneous photo-Fenton degradation of the azo dyes with different structures was conducted in the presence of the amidoximated PAN fiber Fe complex. The QSPR model equations for the dye decoloration and mineralization were successfully developed using MLR technique. MW/S (molecular weight divided by the number of sulphonate groups) and  $N_{N=N}$  (the number of azo linkage) are considered as the most important determining factor for the dye degradation and mineralization, and there is a significant negative correlation between MW/S or  $N_{N=N}$  and degradation percentage or total organic carbon (TOC) removal. Moreover, LOO and CV analysis suggested that the obtained QSPR model equations have the better prediction ability. The variation in Fe content of catalyst and the addition of sodium chloride did not alter the nature of the QSPR model equations.

**Key words:** azo dye; heterogeneous Fenton degradation; quantitative structure property relationship; polyacrylonitrile fiber Fe complex

**DOI:** 10.1016/S1001-0742(12)60190-9

### Introduction

Azo dyes are an abundant class of purely synthetic organic compounds, which are characterized by the presence of one or more azo bonds. Some of them are proven to be potentially carcinogenic and/or teratogenic on public health (Dong et al., 2008). In general, water soluble azo dyes include reactive, acid and direct dyes. They contain water soluble sulphonate groups attached to usually an azobenzenoid chromophore. However, they are dissimilar in many molecular properties such as size, shape and bonding characteristics (Greaves et al., 2001). Water soluble azo dyes are generally considered as the most difficult to remove or degrade from the dyeing effluent, due to their high stability and composition ratio of aromatic rings present in their molecule structure. Therefore, there have been various approaches to destruct them efficiently in aqueous system. In recent years, the heterogeneous Fenton reaction systems as novel advanced oxidation processes (AOPs) have been used for the degradation of the organic

pollutants such as azo dyes in the industrial wastewaters because homogeneous Fenton reactions are found to be the limitation of pH value and the problem of separation and regeneration at the end of the reaction. Moreover, the modified polyacrylonitrile (PAN) fiber Fe complexes have been regarded as one of promising heterogeneous Fenton catalysts because of its unique advantages, such as lower cost and easy preparing and separation of the catalyst after the reaction (Ishtchenko et al., 2003; Han et al., 2011). In order to understand the relationship between the degradation efficiency and molecular structure of organic pollutants it would be more accurate to measure the degradation efficiency for each compound independently, however this would be a cost and time prohibitive prospect (Magnuson et al., 2005). Quantitative structure property relationship (QSPR) have been widely used to examine degradation mechanism and the reactivity of aromatic compounds, especially substituted phenols in AOPs processes (Chen et al., 1996, 1998) because of its conservation of resources by predicting the results of time-consuming and expensive experiments. Chen et al.

\* Corresponding author. E-mail: [teamdong@sina.cn](mailto:teamdong@sina.cn)



(1996, 1998a, 1998b, 2001a, 2001b, 2001c) investigated the photolysis of the aromatic compounds using partial least squares (PLS) method. Kušić et al. (2009) predicted the rate constants for radical degradation of aromatic pollutants in water matrix by genetic algorithm and multiple regression analysis. The degradation of some substituted phenols by singlet oxygen (Tratnyek et al., 1991), ozone (Liu et al., 2010), ultrasound-irradiated Fenton-like system (Zhou et al., 2010), or electrochemical oxidation (Pulgarin et al., 2003; Yuan et al., 2006) was evaluated from QSPR analysis. To define the molecular features that are responsible for the bioelimination of water soluble azo dyes, Churchley et al. (2000, 2001) applied single correlation and multiple linear regression (MLR) method to derive QSPR model and highlighted that the dyes with larger molecular size/ionic charge ratios had the superior levels of bioelimination. Despite numerous applications of QSPR in environmental studies, we are unaware of any attempts to build the QSPR models for degradation of water soluble azo dyes through the heterogeneous Fenton process. In the present study, the amidoximated PAN fiber Fe complexes were first prepared and then used for the catalytic degradation of 28 anionic water soluble azo dyes under visible irradiation. And MLR technique was then applied to develop QSPR models for the dye degradation to investigate the relationship between their degradation efficiency and structure as well as predict the heterogeneous Fenton degradation performance of similar azo dyes.

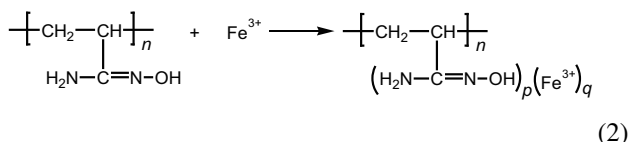
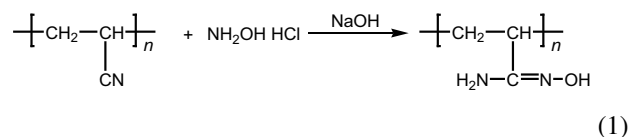
## 1 Materials and methods

### 1.1 Reagents and materials

The commercially available PAN knitting bulky yarn (abbr. PAN yarn) that consisted of twisted PAN fibers were provided by Shanghai Shilin Spinning Co., China. Its content of acrylonitrile was determined and calculated to be 86.96%. Hydroxylamine hydrochloride, ferric chloride, hydrogen peroxide (30%, *m/m*), sodium hydroxide, and sodium chloride were of laboratory grade and purchased from Tianjin Nankai Chemicals Co., China. A total of 28 typical anionic water soluble azo dyes were selected as model pollutants in the current study, mainly because of their relatively high consumption rates in China for textile dyeing processes. All the dyes used were commercially available. They were purified by precipitation from aqueous solution with sodium chloride, and then desalinated using distilled water, finally re-precipitated by the addition of alcohol (Greaves et al., 2001). The purities of all the dyes were evaluated by thin-layer chromatography (TLC) and elemental analysis and were found to be higher than 90% pure. Double distilled and deionized water was used throughout the study.

### 1.2 Preparation of PAN fibrous catalyst

According to our previous works (Dong et al., 2010; Han et al., 2011), PAN fiber was modified with hydroxylamine hydrochloride at 68°C for a given time to introduce amidoxime groups onto the fiber surface. The degree of conversion from nitrile groups to amidoxime groups on the surface of PAN fiber was calculated from the mass gain. And these amidoxime groups were then used to coordinate with 0.10 mol/L FeCl<sub>3</sub> for the given time and under continuous agitation at room temperature to prepare amidoximated PAN fiber Fe complex (Fe-AO-PAN). The residual concentrations of Fe<sup>3+</sup> ions in the solutions after coordination were determined by using a WXF120 atomic absorption spectrometry (Beijing Rayleigh Analytical Instrument Corp., China) for calculating the Fe content ( $Q_{\text{Fe}}$ ) of the complexes. A series of Fe-AO-PAN samples with different  $Q_{\text{Fe}}$  values were then produced by control the coordination time. The two reactions are depicted by Eqs. (1) and (2).



### 1.3 Dye degradation procedure and analysis

The dye degradation was performed in a photoreaction system, which consisted mainly of polished aluminum chamber, lamps, electromagnetic valve, relay and water bath. And the diagram of the photoreaction system was presented in our previous study (Dong et al., 2010). A cut-off filter was used to ensure irradiation only by visible light ( $\lambda > 420$  nm). Light intensity inside photoreaction system was measured to be 9.11 mW/cm<sup>2</sup> using FZ-A radiometer (BNU Light and Electronic Instrumental Co., China), and the temperature in reaction vessel was kept at 25°C. Dye degradation was initialized after the adsorption/desorption equilibrium of the dye on catalyst. The 0.25 g catalyst was placed into 50 mL of test solution containing 0.05 mmol/L dye and 3.0 mmol/L H<sub>2</sub>O<sub>2</sub> at an initial pH of 6.0. The test solution was put under visible irradiation in photoreaction system. At given time intervals, 1–2 mL of the test solution was withdrawn from the reaction vessel and diluted appropriately; the absorbance was then measured at the  $\lambda_{\text{max}}$  of the solution. The concentration of the dye was determined with a UV-2401 Shimadzu spectrophotometer (Shimadzu Co., Japan). The decoloration percentage ( $D$ , %) of the dye was expressed as:

$$D = \left( 1 - \frac{C}{C_0} \right) \times 100\% \quad (3)$$

where,  $C_0$  (mmol/L) is the initial concentration of the dye and  $C$  (mmol/L) is the residual concentration of the dye. Moreover, total organic carbon (TOC) was assayed in the dye degradation process by using a Phoenix 8000 TOC analyzer (Tekmar-Dehmann Inc., USA), and the TOC removal ( $R_T$ , %) of the dye was calculated as follows:

$$R_T = \left(1 - \frac{\text{TOC}_t}{\text{TOC}_0}\right) \times 100\% \quad (4)$$

where,  $\text{TOC}_0$  (mg/L) and  $\text{TOC}_t$  (mg/L) are the TOC values at reaction time 0 and  $t$  (min), respectively.

#### 1.4 Development of QSPR model

Previous studies on the molecular structure of anionic water soluble dyes to their bioelimination by a biomass at wastewater treatment revealed that although 72 molecular descriptors had been useful in the prediction of bioelimination, the factors of  $MW/S$  (molecular weight divided by the number of sulphonate groups),  $N_{N=N}$  (the number of azo linkage), and  $N_{AR}$  (the number of aromatic rings) were found to be three most important molecular descriptors (Greaves et al., 2001; Churchley et al., 2000). Therefore, these three factors were selected as the molecular descriptors in the current study. The inorganic/organic value ( $I/O$  value; inorganic character divided by organic character) was also added as the molecular descriptor and calculated from the molecular structure of each dyes according to the method of Fujita (Fujita, 1954; Nakai et al., 2002), because it has much close relation to the characteristic properties, such as adsorption, dyeing and degradation of the azo dyes in water. Four molecular descriptors for each dye are shown in **Table 1**.

To develop the QSPR models for the heterogeneous Fenton degradation of azo dyes in water, SPSS for Windows (version 19.0) software program was used to build MLR models with default settings. Before performing MLR analysis, the data set was divided into two sub-data sets, one for training, and the other one for testing. In this work, 22 dyes were in training set and 6 dyes in test set. The QSPR model regression equations were found by means of training set, and then the prediction power of which was checked by test set as an external data set. It is should be noticed that the predictive ability of final QSPR models were assessed using Leave-one-out (LOO) and cross-validation (CV) methods in terms of the squared regression coefficient ( $R^2$ ) and the cross-validation correlation coefficient ( $q^2$ ). For external validation, the quality of predictions is judged from the  $q_{\text{ext}}^2$ . They were calculated using Eqs (5) and (6), respectively.

$$q^2 = 1 - \frac{\sum_i^{\text{training}} (y_i - \hat{y}_i)}{\sum_i^{\text{training}} (y_i - \bar{y}_i)} \quad (5)$$

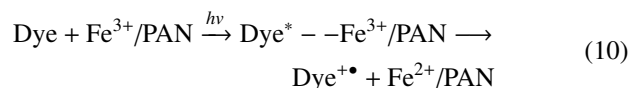
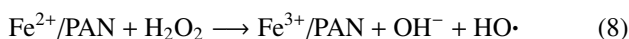
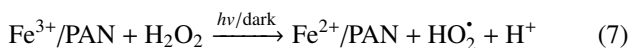
$$q_{\text{ext}}^2 = 1 - \frac{\sum_i^{\text{test}} (y_i - \hat{y}_i)}{\sum_i^{\text{test}} (y_i - \bar{y}_i)} \quad (6)$$

where,  $y_i$  and  $\hat{y}_i$  are observed and predicted values, respectively, and  $\bar{y}_i$  is the average of the observed values in the entire training set data.

## 2 Results and discussion

### 2.1 Heterogeneous Fenton degradation of azo dyes catalyzed by Fe-AO-PAN

Our previous works (Dong et al., 2010; Han et al., 2011) found that Fe-AO-PAN had a significant catalytic ability on heterogeneous Fenton degradation of azo dye with  $\text{H}_2\text{O}_2$  in water, because it could react with  $\text{H}_2\text{O}_2$  to produce OOH radicals. Meanwhile, the reduction of  $\text{Fe}^{3+}$  to  $\text{Fe}^{2+}$  ions loaded was also performed. The resultant  $\text{Fe}^{2+}$  ions combined with  $\text{H}_2\text{O}_2$  to generate OH radicals for dye degradation. On the other hand, the formed  $\text{Fe}^{2+}$  ions on Fe-AO-PAN may be oxidized to become  $\text{Fe}^{4+}$  ions (Kremer, 2003; Groves, 2006), which is also responsible for dye degradation. Additionally, the photosensitization of the azo dyes can promote a conversion of  $\text{Fe}^{3+}$  to  $\text{Fe}^{2+}$  ions during photo-assisted Fenton reaction (Dhananjeyan et al., 2001). These reaction processes are expressed by Reactions (7)–(11).



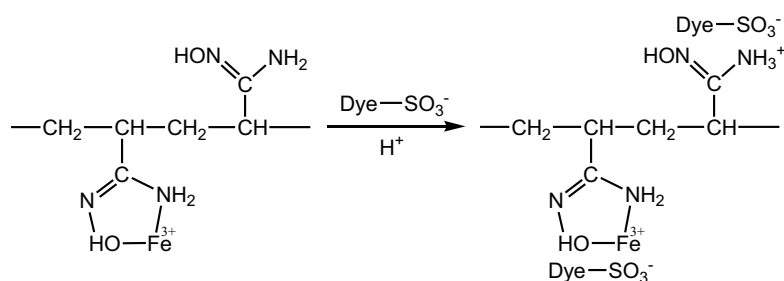
In this study, 22 azo dyes were decomposed with  $\text{H}_2\text{O}_2$  in the presence of Fe-AO-PAN ( $Q_{\text{Fe}} = 1.293$  mmol/g) under visible irradiation, and the  $D$  and  $R_T$  values within 30 min for each dye studied were measured and shown in **Table 1**.

It was evident from **Table 1** that observed  $D$  values were higher than observed  $R_T$  values for all the azo dyes studied, suggesting that their mineralization was carried out with more difficulty than decoloration at the same

**Table 1** Molecular descriptors,  $D$  and  $R_T$  values for 22 azo dyes in the training set.

Dye	Molecular descriptor				$D$ (%)		$R_T$ (%)	
	MW/S	$N_{N=N}$	$N_{AR}$	I/O	Observed	Predicted	Observed	Predicted
Reactive Blue 222	339	2	7	8.53	60.40	57.86	19.57	19.93
Reactive Yellow 145	342	1	5	9.92	62.89	63.67	23.61	23.96
Reactive Red 195	284	1	6	5.69	63.52	64.93	30.93	31.75
Reactive Red 120	245	2	9	5.48	60.23	61.85	33.38	29.23
Reactive Red 2	308	1	4	3.60	62.04	62.57	33.36	29.25
Reactive Red 24	262	1	5	4.69	63.14	65.88	31.52	31.03
Reactive Yellow 86	334	1	3	4.88	63.57	61.75	26.26	25.22
Acid Black 234	431	3	6	3.32	49.92	44.49	5.93	11.89
Acid Red 88	400	1	4	2.5	63.87	56.29	30.41	28.88
Acid Blue 113	340	2	6	2.78	58.56	54.89	26.15	24.00
Acid Red 229	541	2	4	2.25	42.43	42.38	17.57	16.78
Acid Yellow 17	276	1	2	4.73	62.87	65.38	16.15	24.18
Chrome Black 9	382	1	3	3.70	52.34	58.15	29.03	25.69
Acid Orange 156	462	2	3	2.13	48.85	47.33	14.63	16.07
Acid Black 1	308	2	4	3.71	63.01	57.59	25.76	19.15
Direct Blue 71	257	3	8	4.38	55.84	55.60	13.47	18.07
Direct Red 13	356	2	6	3.05	54.96	54.04	19.47	23.43
Direct Black 19	420	4	6	3.22	35.17	40.08	8.05	2.21
Direct Black 17	529	2	4	2.21	39.30	43.10	17.59	17.03
Direct Red 31	357	2	6	3.09	52.80	54.00	23.65	23.37
Direct Blue 15	249	2	6	5.28	63.97	61.84	25.62	22.82
Direct Red 28	348	2	6	2.89	46.77	54.45	16.70	23.74

MW/S: molecular weight divided by the number of sulphonate groups,  $N_{N=N}$ : the number of azo linkage,  $N_{AR}$ : the number of aromatic rings, and I/O: inorganic character divided by organic character.  $D$ : decoloration,  $R_T$ : TOC removal.

**Fig. 1** Adsorption model of azo dye on the surface of Fe-AO-PAN.

conditions. Comparing three classes of azo dyes, reactive dyes generally exhibited the higher observed  $D$  and  $R_T$  values (60%–70% and 20%–30%) than most of the acid and direct dyes. A main reason is that reactive dye molecules often contain more sulphonate groups than the other two dye molecules (Greaves et al., 2001; Churchley et al., 2000). It is necessary to adsorb the reactant molecules strongly enough for them to react, although a good heterogeneous Fenton catalyst should be efficient producing oxidizing species. When Fe-AO-PAN was used as heterogeneous Fenton catalyst in acidic aqueous solution during the degradation, the anionic reactive dye molecule with more sulphonate groups could easily react with cationized amidoxime groups on the surface of Fe-AO-PAN through electrostatic attraction, thus leading to a significant adsorption between them. This adsorption model is described using **Fig. 1**.

## 2.2 QSPR model generation

As mentioned above, the data listed in **Table 1** were used as a training set for the QSPR models. MLR analysis of

the observed  $D$  and  $R_T$  values as well as four molecular descriptors were performed to correlate the parameters with the training set, and based on  $R^2$  and  $q^2$  values. The final QSPR model Eqs. (I) and (II) developed to describe the degradation properties of azo dyes are presented in the following equations.

$$D = -0.0621MW/S - 5.038 N_{N=N} - 0.116N_{AR} + 0.526I/O + 85.28$$

$$N = 22, R^2 = 0.8139, S = 4.196, F = 18.58, P = 0.000, q^2 = 0.6817$$

$$P_{(MW/S)} = 0.000, P_{N=N} = 0.008, P_{AR} = 0.887, P_{I/O} = 0.367 \quad (I)$$

$$R_T = -0.017MW/S - 9.976N_{N=N} + 2.189N_{AR} - 1.092I/O + 39.63$$

$$N = 22, R^2 = 0.7482, S = 4.402, F = 12.63, P = 0.000, q^2 = 0.5070$$

$$P_{MW/S} = 0.281, P_{N=N} = 0.000, P_{AR} = 0.018, P_{I/O} = 0.085 \quad (II)$$

where,  $N$ : number of azo dyes,  $R^2$ : squared regression coefficient,  $q^2$ : cross-validated squared correlation coefficient,  $S$ : standard error of estimate,  $F$ : variance ratio,  $P$ : significance level.

It is found from the above model that for both model Eqs. (I) and (II),  $R^2 > 0.70$  and  $P < 0.05$ , suggesting that both model equations are significant at the 95% confidence

level. In the case of model Eq. (I),  $P_{MW/S}$  and  $P_{N=N}$  values are lower than 0.05, indicating that both MW/S and  $N_{N=N}$  are considered as the most important determining factor for the dye degradation. Moreover, MLR analysis shows there is a significant negative correlation between MW/S or  $N_{N=N}$  and  $D$  value. This means that increasing MW/S and  $N_{N=N}$  lead to a remarkable reduction in the  $D$ . On the contrary, the  $D$  varied insignificantly with  $N_{AR}$  and  $I/O$  values. It is worth noticing that the dyes with more sulphonate groups, especially reactive dyes have a relatively low MW/S, thus showing the higher  $D$  value, which may be the result of enhancing the adsorption between Fe-AO-PAN and dye molecule mentioned above. In the case of model Eq. (II), it is still significant at the 95% confidence level owing to  $R^2 = 0.7482$  and  $P < 0.05$ . MW/S and  $N_{N=N}$  are also the most important determining factor for the dye mineralization. However, it should be pointed out that  $N_{AR}$  has an insignificant enhancing effect on  $R_T$ , while  $I/O$  shows a reverse trend, which is different from the results obtained from model Eq. (I). A possible explanation is that according to references (Zhang et al., 2007; Huang et al., 2004; Konstantinou and Albanis, 2003; Guillard et al., 2003), the degradation pathway of water soluble azo dye with heterogeneous photo-Fenton reaction can be demonstrated using three main steps. The first step is the breaking down of azo and C–N bonds by OH radicals with the formation of aniline-like and phenol-like compounds, thus causing the decoloration. The aromatic rings began to be transformed to multisubstituted benzene at the second step. Meanwhile, the sulphonic groups were cut off from the aromatic rings. The last step is that the aromatic compounds including aniline-like and phenol-like compounds, particularly substituted benzene were oxidized further and mineralized to  $H_2O$  and  $CO_2$ , etc. More importantly, the adsorption of the aromatic intermediates formed on Fe-AO-PAN is essential before the mineralization. And the adsorption between them is highly determined by Van der Waals force due to the breaking off of sulphonic groups. Consequently, it is believed that the aromatic intermediates with more  $N_{AR}$  and less  $I/O$  values may be attracted to Fe-AO-PAN easily, thus leading to their fast mineralization.

### 2.3 Validation of QSPR model

It is observed that  $R^2 > 0.6$  and  $q^2 > 0.5$  for model Eqs. (I) and (II), indicating that both model equations are stable and have high prediction power (Tropsha et al., 2003; Gebhard and Stephen, 2010). Using both model Eqs. (I) and (II), the predicted  $D$  and  $R_T$  values for the training and test sets can be obtained, respectively, as listed in **Tables 1** and **2**. Furthermore, the relationship between the observed and predicted  $D$  and  $R_T$  values obtained by the model Eqs. (I) and (II) is plotted and shown in **Fig. 2**.

**Figure 2** shows that the correlation coefficient ( $R_{tra}^2$ ) between observed and predicted  $D$  and  $R_T$  values for training set by the model Eqs. (I) and (II) are 0.8139

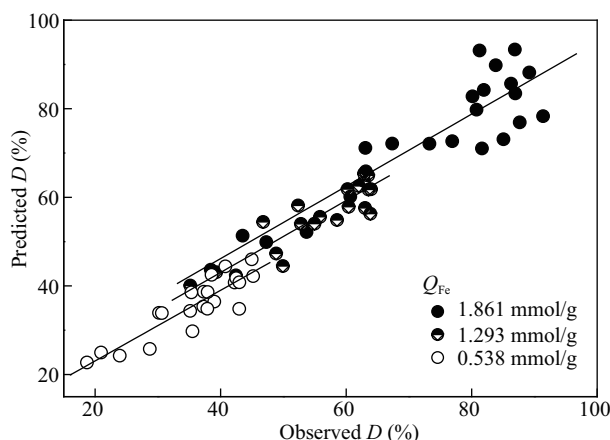


**Fig. 3** A plot of observed and predicted values of  $D$  using three model equations for different  $Q_{Fe}$  (0.538 mmol/g at  $R_{tra}^2 = 0.7938$ , 1.293 mmol/g at  $R_{tra}^2 = 0.8139$ ; 1.861 mmol/g at  $R_{tra}^2 = 0.8146$ ).

and 0.7482, respectively, which proposes that both model equations are significant. For external validation with test set, the quality of predictions is generally judged from the  $q_{ext}^2$  value. For a predictive QSPR model, the value of  $q_{ext}^2$  should be more than 0.5 (Ojha et al., 2011). Therefore, the model Eqs. (I) and (II) are considered acceptable since  $R_{ext}^2 = 0.9326$ ,  $q_{ext}^2 = 0.8360$  for  $D$  values and  $R_{ext}^2 = 0.8431$ ,  $q_{ext}^2 = 0.7215$  for  $R_T$  values presented in **Fig. 2** and **Table 2**.

### 2.4 Effect of Fe content of Fe-AO-PAN

The degradation of 22 azo dyes in training set was conducted in the presence of Fe-AO-PAN with different  $Q_{Fe}$  values under visible irradiation, and their  $D$  values within 30 min were measured and used for generating QSPR models (**Table 3**).

It is evident from model Eqs. (III) and (IV) are still significant at the 95% confidence level because their  $R^2$  values (0.8244 for Eq. (III), 0.8154 for Eq. (IV)) are higher, and  $P$  values are much less than 0.05. Moreover,  $P_{MW/S}$  and  $P_{N=N}$  values are lower than 0.05 for model Eqs. (III) and (IV), demonstrating that both MW/S and  $N_{N=N}$  are considered as the most important determining factor for the dye degradation. These results imply that Fe content of Fe-AO-PAN does not alter the nature of the quantitative relationship of dye structure and their degradation performance. On the other hand, the predicted  $D$  values for the training set can be calculated through three model Eqs. (III), (I) and (IV), respectively, and then the graphical correlation between the observed and predicted  $D$  values is presented in **Fig. 3**.

**Figure 3** and **Table 3** shows that the  $R_{tra}^2$  was relatively high, and  $q^2$  values are larger than 0.50 for model equations (III) and (IV), suggesting the model QSPR equations obtained when Fe-AO-PAN with different  $Q_{Fe}$  values being used as the heterogeneous Fenton catalysts are robust. **Figure 3** also shows that increasing  $Q_{Fe}$  of Fe-AO-PAN from 0.538 to 1.861 mmol/g is accompanied with a significant enhancement in  $D$  for each dye. This is attributed to



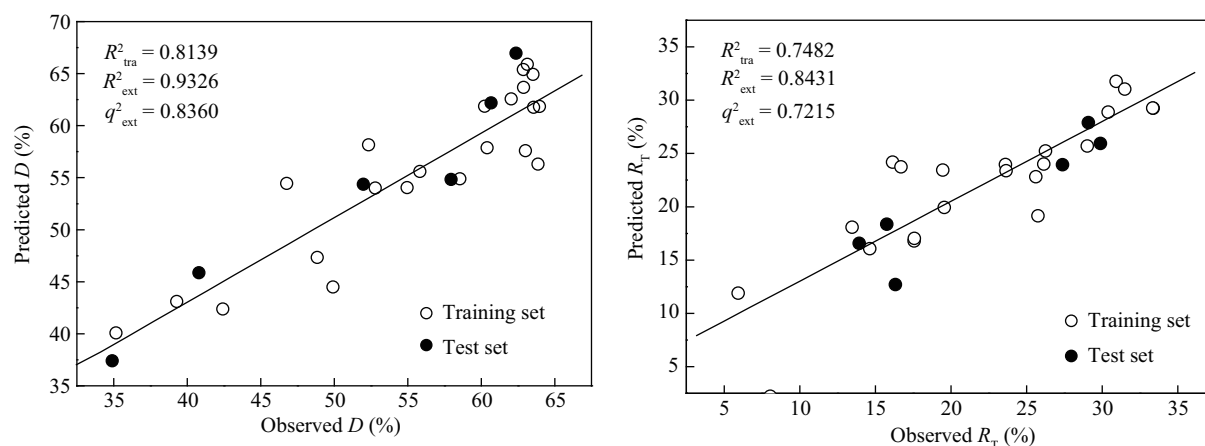


Fig. 2 Relationship between the observed and predicted  $D$  or  $R_T$  values.

more active sites on the surface of Fe-AO-PAN with higher  $Q_{Fe}$ , which can promote the  $H_2O_2$  decomposition and produce high concentration of OH radicals is responsible for dye degradation (Dong et al., 2010).

### 2.5 Effect of sodium chloride

Dyeing of textiles with azo dyes is significantly improved by the addition of inorganic salts, especially sodium chloride, but which increase pollution load on dyehouse effluent in general (Perkins, 2004). In this approach, the photocatalytic decoloration of the azo dyes was carried out in the presence or absence of sodium chloride (40.0 g/L) under visible light for investigating the effect of sodium chloride on the QSPR model equation, and the results were shown in Table 4 and Fig. 4.

It is clear from Table 4 that the model Eq. (V) has the similar  $R^2$ ,  $P$ ,  $P_{(MW/S)}$  and  $P_{N=N}$  values to those of model Eq. (IV), indicating that it is also of significance at the 95% confidence level, and the azo dye degradation is greatly determined by MW/S and  $N_{N=N}$  as the two most important molecular descriptors. Besides, it is noticed in Table 4 and Fig. 4 that the model Eq. (V) possesses a little higher  $R^2_{tra}$  and  $q^2$  values than those of model Eq. (IV), implying that it regarded as a better predictive model equation. Therefore, it is concluded that the presence of sodium chloride causes a very limited impact on the nature of QSPS model equation developed and its prediction power. However, Fig. 4 shows that the addition of sodium

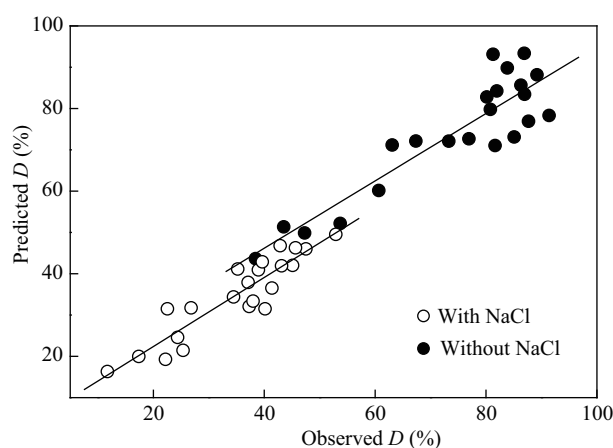


Fig. 4 A plot of observed and predicted  $D$  values using the two model equations with and without salt (with NaCl at  $R^2_{tra} = 0.8352$ , without NaCl at  $R^2_{tra} = 0.8146$ ).

chloride leads to a dramatic reduction in the  $D$  of all the azo dye examined. This mainly is due to the hydroxyl radical scavenging effect of chloride ion and enhanced aggregation and limited ionization of dye molecules in water (Dong et al., 2007).

### 3 Conclusions

The amidoximated PAN fiber Fe complexes could be used as the heterogeneous Fenton catalysts for the degradation

Table 2 Molecular descriptors,  $D$  and  $R_T$  values for 6 azo dyes in the test set

Dye	Molecular descriptors				$D$ (%)		$R_T$ (%)	
	MW/S	$N_{N=N}$	$N_{AR}$	$I/O$	Observed	Predicted	Observed	Predicted
Reactive Red 261	441	1	5	4.78	57.96	54.83	29.1	27.89
Reactive Black 5	248	2	4	5.37	60.67	62.18	15.76	18.36
Acid Red 1	255	1	3	5.46	62.37	66.95	29.9	25.93
Acid Blue 120	348	2	6	2.72	51.99	54.36	27.38	23.93
Direct Green 6	406	3	6	2.97	40.80	45.86	16.33	12.69
Direct Brown 2	627	2	5	3.12	34.91	37.39	13.94	16.56

MW/S: molecular weight divided by the number of sulphonate groups,  $N_{N=N}$ : the number of azo linkage,  $N_{AR}$ : the number of aromatic rings, and  $I/O$ : inorganic character divided by organic character.

**Table 3** Effect of  $Q_{Fe}$  value on QSPR model equations

$Q_{Fe}$	QSPR model equations and statistical values
0.538 mmol/g	$D = -0.060MW/S - 3.698N_{N=N} - 0.804N_{AR} + 0.220I/O + 66.83$ $N = 22, R^2 = 0.8244, S = 3.784, F = 16.36, P = 0.000, q^2 = 0.6571$ $P_{MW/S} = 0.000, P_{N=N} = 0.026, P_{AR} = 0.280, P_{I/O} = 0.673$ (III)
1.293 mmol/g	$D = -0.0621MW/S - 5.038N_{N=N} - 0.116N_{AR} + 0.526I/O + 85.28$ $N = 22, R^2 = 0.8138, S = 4.196, F = 18.58, P = 0.000, q^2 = 0.6817$ $P_{MW/S} = 0.000, P_{N=N} = 0.008, P_{AR} = 0.887, P_{I/O} = 0.367$ (I)
1.861 mmol/g	$D = -0.122MW/S - 9.847N_{N=N} - 0.649N_{AR} + 0.013I/O + 138.1$ $N = 22, R^2 = 0.8154, S = 7.642, F = 18.66, P = 0.000, q^2 = 0.7122$ $P_{MW/S} = 0.000, P_{N=N} = 0.005, P_{AR} = 0.661, P_{I/O} = 0.990$ (IV)

**Table 4** QSPR model equations in the presence or absence of sodium chloride

Conditions	QSPR model equations and statistical values
With NaCl	$D = -0.064 MW/S - 5.673N_{N=N} - 0.452N_{AR} + 1.606I/O + 63.43$ $N = 22, R^2 = 0.8354, S = 4.813, F = 21.54, P = 0.000, q^2 = 0.7423$ $P_{MW/S} = 0.001, P_{N=N} = 0.009, P_{AR} = 0.628, P_{I/O} = 0.025$ (V)
Without NaCl	$D = -0.122 MW/S - 9.847N_{N=N} - 0.649N_{AR} + 0.013I/O + 138.1$ $N = 22, R^2 = 0.8154, S = 7.643, F = 18.66, P = 0.000, q^2 = 0.7122$ $P_{MW/S} = 0.000, P_{N=N} = 0.005, P_{AR} = 0.661, P_{I/O} = 0.990$ (IV)

of 28 anionic water soluble azo dyes with different structures in water under visible irradiation. Generally, reactive dyes showed the higher decoloration and mineralization performance than most of the acid and direct dyes. The QSPR model equations for the dye decoloration and mineralization were successfully developed using MLR technique. QSPR analysis indicated that both MW/S and  $N_{N=N}$  are considered as the most important determining factor for the dye degradation and mineralization, and there is a significant negative correlation between MW/S or  $N_{N=N}$  and degradation percentage or TOC removal. Moreover, LOO and CV analysis demonstrated that the obtained QSPR model equations have the better prediction ability for the heterogeneous Fenton degradation performance of the anionic water soluble azo dyes. Besides, although the variation in Fe content of catalyst and the addition of sodium chloride led to a significant change in dye degradation, however, these variables did not alter the nature of the QSPR model equations. Therefore, these QSPR model equations obtained should be useful not only to understand the relationship between degradation property and structure of the azo dyes, but also to design the environmental-friendly azo dyes for the textile industry.

### Acknowledgments

This work was supported by the Research Program of Application Foundation and Advanced Technology from the Tianjin Municipal Science and Technology Committee (No. 11JCZDJ24600) and the Natural Science Foundation of China (No. 20773093).

### References

- Chen J W, Kong L R, Zhu C M, Huang Q G, Wang L S, 1996. Correlation between photolysis rate constants of polycyclic aromatic hydrocarbons and frontier molecular orbital energy. *Chemosphere*, 33(6): 1143–1150.
- Chen J W, Peijnenburg W J G M, Quan X, Chen S, Martens D, Schramm K W, Kettrup A, 2001a. Is it possible to develop a QSPR model for direct photolysis half-lives of PAHs under irradiation of sunlight? *Environmental Pollution*, 114(1): 137–143.
- Chen J W, Peijnenburg W J G M, Quan X, Zhao Y Z, Xue D M, Yang F L, 1998a. The application of quantum chemical and statistical technique in developing quantitative structure-property relationships for the photohydrolysis quantum yields of substituted aromatic halides. *Chemosphere*, 37(6): 1169–1186.
- Chen J W, Peijnenburg W J G M, Wang L S, 1998b. Using PM3 Hamiltonian, factor analysis and regression analysis in developing quantitative structure-property relationships for photohydrolysis quantum yields of substituted aromatic halides. *Chemosphere*, 36(13): 2833–2853.
- Chen J W, Quan X, Peijnenburg W J G M, Yang F L, 2001b. Quantitative structure-property relationships (QSPRs) on direct photolysis quantum yields of PCDDs. *Chemosphere*, 43(1): 235–241.
- Chen J W, Quan X, Yan Y, Yang F L, Peijnenburg W J G M, 2001c. Quantitative structure-property relationship studies on direct photolysis of selected polycyclic aromatic hydrocarbons in atmospheric aerosol. *Chemosphere*, 42(3): 263–270.
- Churchley J H, Greaves A J, Hutchings M G, Phillips D A S, Taylor J A, 2000. A chemometric approach to understanding the bioelimination of anionic, water-soluble dyes by a biomass-Part 4: Reactive dyes. *Coloration Technology*,

- 116(10): 323–329.
- Dhananjeyan M R, Kiwi J, Albers P, Enea O, 2001. Photo-assisted immobilized Fenton degradation up to pH 8 of azo dye Orange II mediated by Fe<sup>3+</sup>/Nafion/glass fibers. *Helvetica Chimica Acta*, 84(11): 3433–3445.
- Dong Y C, Chen J L, Li C H, Zhu H X, 2007. Decoloration of three azo dyes in water by photocatalysis of Fe (III) oxalate complexes/H<sub>2</sub>O<sub>2</sub> in the presence of inorganic salts. *Dyes and Pigments*, 73(2): 261–268.
- Dong Y C, Han Z B, Liu C Y, Du F, 2010. Preparation and photocatalytic performance of Fe(III)-amidoximated PAN fiber complex for oxidative degradation of azo dye under visible light irradiation. *Science of the Total Environment*, 408(10): 2245–2253.
- Dong Y C, He L C, Yang M, 2008. Solar degradation of two azo dyes by photocatalysis using Fe(III)-oxalate complexes/H<sub>2</sub>O<sub>2</sub> under different weather conditions. *Dyes and Pigments*, 77(2): 343–350.
- Fujita A, 1954. Prediction of organic compounds by a conceptual diagram. *Pharmaceutical Bulletin, Tokyo Pharmaceutical Society of Japan*, 2(2): 163–173.
- Gebhard B L, Stephen E C, 2010. Quantitative structure-property relationship for predicting chlorine demand by organic molecules. *Environmental Science and Technology*, 44(7): 2503–2508.
- Greaves A J, Churchley J H, Hutchings M G, Phillips D A S, Taylor J A, 2001. A chemometric approach to understanding the biodegradation of anionic, water-soluble dyes by a biomass using empirical and semi-empirical molecular descriptors. *Water Research*, 35(5): 1225–1239.
- Groves J T, 2006. High-valent iron in chemical and biological oxidations. *Journal of Inorganic Biochemistry*, 100(4): 434–447.
- Guillard C, Lachheb H, Houas A, Ksibi M, Elaloui E, Hermann J M, 2003. Influence of chemical structure of dyes, of pH and of inorganic salts on their photocatalytic degradation by TiO<sub>2</sub> comparison of the efficiency of powder and supported TiO<sub>2</sub>. *Journal of Photochemistry and Photobiology A: Chemistry*, 158(1): 27–36.
- Han Z B, Dong Y C, Dong S M, 2011. Copper-iron bimetal modified PAN fiber complexes as novel heterogeneous Fenton catalysts for degradation of organic dye under visible light irradiation. *Journal of Hazardous Materials*, 189(1-2): 241–248.
- Huang Y P, Li J, Ma W H, Cheng M M, Zhao J C, 2004. Efficient H<sub>2</sub>O<sub>2</sub> oxidation of organic pollutants catalyzed by supported iron sulfophenylporphyrin under visible light irradiation. *Journal of Physical Chemistry B*, 108(22): 7263–7270.
- Ishtchenko V V, Huddersman K D, Vitkovskaya R F, 2003. Part I. Production of a modified PAN fibrous catalyst and its optimisation towards the decomposition of hydrogen peroxide. *Applied Catalysis A: General*, 242(1): 123–137.
- Konstantinou I K, Albanis T A, 2003. Photocatalytic transformation of pesticides in aqueous titanium dioxide suspensions using artificial and solar light: intermediates and degradation pathways. *Applied Catalysis B: Environmental*, 42(4): 319–335.
- Kremer M L, 2003. The Fenton reaction. Dependence of the rate on pH. *Journal of Physical Chemistry A*, 107(11): 1734–1741.
- Kuši H, Rasulev B, Leszczynska D, Leszczynski J, Koprivanac N, 2009. Prediction of rate constants for radical degradation of aromatic pollutants in water matrix: A QSAR study. *Chemosphere*, 75(8): 1128–1134.
- Liu H, Tan J, Yu H X, Liu H X, Wang L S, Wang Z Y, 2010. Determination of the apparent reaction rate constants for ozone degradation of substituted phenols and QSPR/QSAR analysis. *International Journal of Environmental Research*, 4(3): 507–512.
- Magnuson M L, Speth T F, 2005. Quantitative structure-property relationships for enhancing predictions of synthetic organic chemical removal from drinking water by granular activated carbon. *Environmental Science and Technology*, 39(19): 7706–7711.
- Nakai S, Saito S, Takeuchi M, Takimoto Y, Matsuo M, 2002. The inorganic and organic characters for predicting bioconcentration on wide variety of chemicals in fish. *SAR and QSAR in Environmental Research*, 13(7-8): 667–673.
- Ojha P K, Mitra I, Das R N, Roy K, 2011. Further exploring  $r_m^2$  metrics for validation of QSPR models. *Chemometrics and Intelligent Laboratory Systems*, 107(1): 194–205.
- Perkins W S, 2004. Textile Coloration and Finishing. Chinese notation edition authorized by Carolina Academic Press, China Textile Press, Beijing. 102–103.
- Pulgarin C, Parra S, Olivero J, Pacheco L, 2003a. Structural properties and photoreactivity relationships of substituted phenols in TiO<sub>2</sub> suspensions. *Applied Catalysis B: Environmental*, 43(3): 293–301.
- Ulgarin C, Ricardo A T, Walter T, Paul P, 2003b. Electrochemical degradation of *p*-substituted phenols of industrial interest on Pt electrodes: Attempt of a structure-reactivity relationship assessment. *Chemosphere*, 50(1): 97–104.
- Tratnyek P G, Holgne J, 1991. Oxidation of substituted phenols in the environment: a QSAR analysis of rate constants for reaction with singlet oxygen. *Environmental Science and Technology*, 25(9): 1596–1602.
- Tropsha A, Gramatica P, Gomba V K, 2003. The Importance of being earnest: Validation is the absolute essential for successful application and interpretation of QSPR model. *QSAR and Combinatorial Science*, 23(1): 69–77.
- Yuan S, Xiao M, Zheng G, Tian M, Lu X, 2006. Quantitative structure-property relationship studies on electrochemical degradation of substituted phenols using a support vector machine. *SAR and QSAR in Environmental Research*, 17(5): 473–481.
- Zhang Y, Dou X M, Liu J, Yang M, Zhang L P, Kamagata Y, 2007. Decolorization of Reactive Brilliant Red X-3B by heterogeneous photo-Fenton reaction using an Fe-Ce bimetal catalyst. *Catalysis Today*, 126(3-4): 387–393.
- Zhou T, Lu X H, Lim T, Li Y Z, Wong F S, 2010. Degradation of chlorophenols (CPs) in an ultrasound-irradiated Fenton-like system at ambient circumstance: The QSPR (quantitative structure-property relationship) study. *Chemical Engineering Journal*, 156(2): 347–352.

# JOURNAL OF ENVIRONMENTAL SCIENCES

环境科学学报(英文版)  
(<http://www.jesc.ac.cn>)

## Aims and scope

*Journal of Environmental Sciences* is an international academic journal supervised by Research Center for Eco-Environmental Sciences, Chinese Academy of Sciences. The journal publishes original, peer-reviewed innovative research and valuable findings in environmental sciences. The types of articles published are research article, critical review, rapid communications, and special issues.

The scope of the journal embraces the treatment processes for natural groundwater, municipal, agricultural and industrial water and wastewaters; physical and chemical methods for limitation of pollutants emission into the atmospheric environment; chemical and biological and phytoremediation of contaminated soil; fate and transport of pollutants in environments; toxicological effects of terrorist chemical release on the natural environment and human health; development of environmental catalysts and materials.

## For subscription to electronic edition

Elsevier is responsible for subscription of the journal. Please subscribe to the journal via <http://www.elsevier.com/locate/jes>.

## For subscription to print edition

China: Please contact the customer service, Science Press, 16 Donghuangchenggen North Street, Beijing 100717, China. Tel: +86-10-64017032; E-mail: [journal@mail.sciencep.com](mailto:journal@mail.sciencep.com), or the local post office throughout China (domestic postcode: 2-580).

Outside China: Please order the journal from the Elsevier Customer Service Department at the Regional Sales Office nearest you.

## Submission declaration

Submission of an article implies that the work described has not been published previously (except in the form of an abstract or as part of a published lecture or academic thesis), that it is not under consideration for publication elsewhere. The submission should be approved by all authors and tacitly or explicitly by the responsible authorities where the work was carried out. If the manuscript accepted, it will not be published elsewhere in the same form, in English or in any other language, including electronically without the written consent of the copyright-holder.

## Submission declaration

Submission of the work described has not been published previously (except in the form of an abstract or as part of a published lecture or academic thesis), that it is not under consideration for publication elsewhere. The publication should be approved by all authors and tacitly or explicitly by the responsible authorities where the work was carried out. If the manuscript accepted, it will not be published elsewhere in the same form, in English or in any other language, including electronically without the written consent of the copyright-holder.

## Editorial

Authors should submit manuscript online at <http://www.jesc.ac.cn>. In case of queries, please contact editorial office, Tel: +86-10-62920553, E-mail: [jesc@263.net](mailto:jesc@263.net), [jesc@rcees.ac.cn](mailto:jesc@rcees.ac.cn). Instruction to authors is available at <http://www.jesc.ac.cn>.

## Journal of Environmental Sciences (Established in 1989)

Vol. 25 No. 7 2013

<b>Supervised by</b>	Chinese Academy of Sciences	<b>Published by</b>	Science Press, Beijing, China
<b>Sponsored by</b>	Research Center for Eco-Environmental Sciences, Chinese Academy of Sciences	<b>Distributed by</b>	Elsevier Limited, The Netherlands
<b>Edited by</b>	Editorial Office of Journal of Environmental Sciences P. O. Box 2871, Beijing 100085, China Tel: 86-10-62920553; <a href="http://www.jesc.ac.cn">http://www.jesc.ac.cn</a> E-mail: <a href="mailto:jesc@263.net">jesc@263.net</a> , <a href="mailto:jesc@rcees.ac.cn">jesc@rcees.ac.cn</a>	<b>Domestic</b>	Science Press, 16 Donghuangchenggen North Street, Beijing 100717, China Local Post Offices through China
<b>Editor-in-chief</b>	Hongxiao Tang	<b>Foreign</b>	Elsevier Limited <a href="http://www.elsevier.com/locate/jes">http://www.elsevier.com/locate/jes</a>
<b>CN 11-2629/X</b>	<b>Domestic postcode: 2-580</b>	<b>Printed by</b>	Beijing Beilin Printing House, 100083, China
		<b>Domestic price per issue</b>	<b>RMB ¥ 110.00</b>

ISSN 1001-0742

